

# Dependence on supernovae light-curve processing in void models

Gabriel R. Bengochea<sup>1,\*</sup> and Maria E. De Rossi<sup>1,2,†</sup>

<sup>1</sup>*Instituto de Astronomía y Física del Espacio (IAFE),  
UBA-CONICET, CC 67, Suc. 28, 1428 Buenos Aires, Argentina*

<sup>2</sup>*Departamento de Física, Facultad de Ciencias Exactas y Naturales, Universidad de Buenos Aires, Argentina*

In this work, we show that when supernova Ia (SN Ia) data sets are used to put constraints on the free parameters of inhomogeneous models, certain extra information regarding the light-curve fitter used in the supernovae Ia luminosity fluxes processing should be taken into account. We found that the size of the void as well as other parameters of these models might be suffering extra degenerations or additional systematic errors due to the fitter. A recent proposal to relieve the tension between the results from Planck satellite and SNe Ia is re-analyzed in the framework of these subjects.

## I. INTRODUCTION

According to a homogeneous and isotropic Friedmann-Robertson-Walker (FRW) standard model, since 1998 combined observations of nearby and distant type Ia supernovae (SNe Ia) led to the discovery of the accelerating universe picture. We now have a *concordance model* in which the dimming of distant SNe Ia [1–10], anisotropies in the cosmic microwave background (CMB) [11, 12], and the signature of baryon acoustic oscillation (BAO) [13, 14] cannot be explained by considering only baryonic and dark matter. The most popular solution is to introduce an additional component with negative pressure, the so-called dark energy (e.g., [15–19]).

Some other proposals have been presented since then. Among them, exact inhomogeneous models with no dark energy component were put forward shortly after the release of the first supernova measurements [20–23]; and more recently some models, such as the ones based on spherically symmetric Lemaître-Tolman-Bondi (LTB) and other exact solutions, began to have an important development in the past few years (see for example, [24–32]). Until today, these have been considered toy-models because of their simplicity and it is necessary to remark that they are not robust models of our universe yet. According to some authors (e.g. [33, 34]), LTB models face important observational challenges and the most simple current versions of these models would be ruled out. As it has been emphasized in the literature, their use must be considered as a mere first step towards more sophisticated models [31]. Examples somewhat more complex are the ones known as Swiss-cheese models [35], meatball models [36] and Szekeres Swiss-cheese models [37]. Note that LTB model breaks the Copernican principle, by placing the observer at the centre of a spherically symmetric universe, while other models, such as the Swiss-cheese one, are only locally inhomogeneous. For a detailed review of exact solutions, see [29].

The importance of the study of aforementioned models is motivated by different observational works. In particular, [38] concluded that local measurements of the near-infrared luminosity density are consistent with models that invoke a large local under-density (around 300 Mpc) to explain either the apparent acceleration observed via type Ia supernovae, or to explain the discrepancy between local measurements of  $H_0$  and those inferred from the CMB. The use of inhomogeneous models is also well justified even in the standard paradigm. For example, it has already been demonstrated that although the cosmological observations are analyzed in the homogeneous framework, matter inhomogeneities might be mistaken for evolving dark energy [39, 40]. Other authors have studied how the presence of a local spherically symmetric inhomogeneity can affect apparent cosmological observables derived from the luminosity distance. Under the assumption that the real space-time is exactly homogeneous and isotropic, they have found that phantom dark energy or quintessence behaviors can be produced for compensated underdense or overdense regions [41]. The fact of putting observational constraints on these type of models should not be taken to be ruled out or not, but as a beacon to follow, and to study possible degenerations present that might influence future works with more refined proposals.

The possible tension between the best fits for  $\Omega_m$  and  $H_0$  obtained from the *Planck* satellite observations on one hand, and the Hubble diagram of SNe Ia on the other hand, has been recently faced by the authors in [42]. They showed that the use of an inhomogeneous Swiss-cheese model to interpret the Hubble diagram allows to reconcile it with *Planck* results.

The flux measurements from an SN Ia at different epochs and distinct passbands are processed with the so-called *light-curve fitters* to obtain luminosity distance values. The two most used methods are named MLCS2k2 [43] (hereafter MLCS) and SALT2 [44]. Distance moduli calculated for the same objects by the two fitting methods are not necessarily equal.

MLCS (The Multicolor Light Curve Shape fitter), is the most recent version of the fitter used by the High-z Supernova Team [2], whilst the SALT2 (Spectral Adap-

\*Electronic address: gabriel@iafe.uba.ar

†Electronic address: derossi@iafe.uba.ar

tive Light curve Template), is an improved version of the fitter used originally by the Supernova Cosmology Project [1]. A detailed description of both fitters and a thorough discussion about systematic errors in SN surveys can be found for example in [4, 5].

It is a known fact that the same SN Ia data set from which distance estimates are analyzed with two different light-curve fitters, can lead to different values for various cosmological parameters, or also some cosmological models would be more favored than others (e.g. [4, 5, 45–49]). One of us, has recently shown how these two light-curve fitters employed for the same SN Ia data set produce the same result than two different SN Ia sets, and it should be minded as an additional factor to decide whether phantom type models are favored or not [50].

Whereas the MLCS calibration uses a nearby training set of SNe Ia assuming a close to linear Hubble law, SALT2 uses the whole data set to calibrate empirical light curve parameters. SNe Ia beyond the range in which the Hubble law is linear are used, so a cosmological model must be assumed in the latter. Typically a  $\Lambda$ CDM or a  $w$ CDM ( $w = \text{const}$ ) model is assumed. Consequently, the published values of SN Ia distance moduli obtained with SALT2 fitter retain a degree of model dependence. Regarding this issue, in [51] it was pointed out that systematic errors in the method of SNe Ia distance estimation have come into sharper focus as a limiting factor in SN cosmology. The major systematic concerns for supernova distance measurements are errors in correcting for host-galaxy extinction and uncertainties in the intrinsic colors of supernovae, luminosity evolution, U-band rest frame in the low-redshift sample and selection bias. Also, SALT2 fitter does not provide a cosmology-independent distance estimate for each supernova, since some parameters in the calibration process are determined in a simultaneous fit with cosmological parameters to the Hubble diagram. It is important to remark that a 0.2 apparent magnitude difference leads to a 10% error in the luminosity distance value. Some researchers have focused on these issues, and important steps have begun to be taken (e.g. [10, 52–64]). Unfortunately, these subjects have been boarded, mostly, just from the SALT2 point of view. Another recently developed light-curve fitter is SiFTO [65]. Although SiFTO differs from SALT2 in some aspects including improvements with respect to the latter, SiFTO shares more features with SALT2 than with MLCS (see for example [7]). In fact, results from SiFTO are finally mostly compared using SALT2 as a guide, and the general conclusion is that the differences associated with these two fitters are not very significant (e.g [7, 65]).

Since in the inhomogeneous framework literature the possible effects of the mentioned issues have been scarcely studied; and stimulated by the approach given by [42], in this Letter, we first analyze the consistency of two of the main light-curve fitters used for the elaboration of SN Ia data sets in the void models framework. To accomplish this, we present a study about the possible results that can be obtained regarding, for instance, the

size of the void; or degenerations in other parameters that are usually used in this type of models, to parameterize their profiles or diagnose when viewed as effective models. We also explore the impact of some systematics induced by the mentioned fitters in such models, to then study how this could affect previous proposals in the literature.

Additionally, we propose that the solution found by the authors in [42] might be even more reinforced if the most recent SNe Ia data were used in the MLCS fitter framework.

## II. THE UNIVERSE ACCORDING TO VOID MODELS

### A. Lemaître-Tolman-Bondi model

Among the variety of papers regarding inhomogeneous models published in the last few years, we chose to follow [66] because of the clarity and detail in the presented results, and because our aim is to show the analysis under consideration in the framework of a simple model.

Then, following the notation of Section 2 of the mentioned work, we will describe the observable universe, for this first case studied, considering an inhomogeneous void centered around us and adopting a spherically symmetric Lemaître-Tolman-Bondi (LTB) model which metric is given by

$$ds^2 = -dt^2 + \frac{a_{||}^2(t, r)}{1 - k(r)r^2} dr^2 + a_{\perp}^2(t, r)r^2 d\Omega^2 \quad (1)$$

where the angular ( $a_{\perp}$ ) and the radial ( $a_{||}$ ) scale factors are related by

$$a_{||} \equiv (a_{\perp} r)' \quad (2)$$

and a prime denotes partial derivative with respect to coordinate distance  $r$ . The curvature  $k(r)$  is not constant but is instead a free function. The coordinates are chosen such that the angular scale factor is constant and satisfies  $a_{\perp}(t_0, r) = 1$  at present epoch. From both scale factors, we can define two Hubble rates,

$$H_{\perp} = H_{\perp}(t, r) \equiv \frac{\dot{a}_{\perp}}{a_{\perp}}, \quad H_{||} = H_{||}(t, r) \equiv \frac{\dot{a}_{||}}{a_{||}} \quad (3)$$

where an over-dot indicates partial differentiation with respect to  $t$ . When the parameters are evaluated to the time today we designate them as  $H_{\perp 0} = H_{\perp 0}(r) = H_{\perp}(t_0, r)$  etc. The Friedmann equation in this geometry is written as

$$H_{\perp}^2 = \frac{M^3}{a_{\perp}} - \frac{k}{a_{\perp}^2}, \quad (4)$$

where  $M(r)$  is another free function of  $r$ , and the locally measured energy density is

$$8\pi G\rho(t, r) = \frac{(Mr^3)_{,r}}{a_{||}a_{\perp}^2 r^2} \quad (5)$$

which satisfies the conservation equation

$$\dot{\rho} + (2H_{\perp} + H_{\parallel}) \rho = 0 \quad (6)$$

Similarly, as in the case of the FRW models, the dimensionless density parameters for the curvature and matter are defined as

$$\begin{aligned} \Omega_k(r) &= -\frac{k}{H_{\perp 0}^2} \\ \Omega_m(r) &= \frac{M}{H_{\perp 0}^2} \end{aligned} \quad (7)$$

so, the Friedmann equation takes the known form:

$$\frac{H_{\perp}^2}{H_{\perp 0}^2} = \Omega_m a_{\perp}^{-3} + \Omega_k a_{\perp}^{-2} \quad (8)$$

in such way that  $\Omega_m(r) + \Omega_k(r) = 1$  is satisfied. Integrating the Friedmann equation from the big bang time  $t_B = t_B(r)$  to some later time  $t$ , the age of the universe at a given  $(t, r)$  can be obtained by,

$$\tau(t, r) = t - t_B = \frac{1}{H_{\perp 0}(r)} \int_0^{a_{\perp}(t, r)} \frac{dx}{\sqrt{\Omega_m(r)x^{-1} + \Omega_k(r)}} \quad (9)$$

We set  $t_B = 0$  so our model evolves from a perturbed FRW model at early times. This way, the age of the universe  $\tau$  is constant, and equal to the time today  $t_0$ . Solving (9) for  $H_{\perp 0}(r)$ , and for the case in which  $\Omega_k > 0$ , we have:

$$H_{\perp 0}(r) = \frac{\sqrt{\Omega_k} - \Omega_m \sinh^{-1} \sqrt{\frac{\Omega_k}{\Omega_m}}}{t_0 \Omega_k^{3/2}} \quad (10)$$

We will use the notation for the Hubble constant  $H_0 = H_{\perp 0}(r = 0)$ , which fixes  $t_0$  in terms of  $H_0$ ,  $\Omega_m(r = 0)$  and  $\Omega_k(r = 0)$ .

Following [25, 66], on the past light cone a central observer may write the  $(t, r)$  coordinates as functions of redshift  $z$ . These functions are determined by the differential equations,

$$\frac{dt}{dz} = -\frac{1}{(1+z)H_{\parallel}} \quad (11)$$

$$\frac{dr}{dz} = \frac{\sqrt{1 - kr^2}}{(1+z)a_{\parallel}H_{\parallel}} \quad (12)$$

where  $H_{\parallel}(t, r) = H_{\parallel}(t(z), r(z)) = H_{\parallel}(z)$ , etc. The area distance is given by

$$d_A(z) = a_{\perp}(t(z), r(z)) r(z) \quad (13)$$

and the luminosity distance is  $d_L(z) = (1+z)^2 d_A(z)$ . With these quantities, the distance modulus is given by

$$\mu(z) = m - \mathcal{M} = 5 \log_{10} \left[ \frac{d_L(z)}{1 \text{ Mpc}} \right] + 25 \quad (14)$$

where  $m$  is the apparent magnitude of a source which absolute magnitude is  $\mathcal{M}$ .

For our LTB case analysis, we chose the model 3 of [66] whose void profile parametrization is given by:

$$\Omega_m(r) = \Omega_{\text{out}} - (\Omega_{\text{out}} - \Omega_{\text{in}}) \frac{\sigma^2}{\sigma^2 + r^2} \quad (15)$$

In the last equation,  $\Omega_{\text{in}}$  is the value of  $\Omega_m$  at the center of the void. As in the cited paper, we fixed  $\Omega_{\text{out}} = 1$ , so that the space is asymptotically flat. This choice, for us, is yet less relevant than for the authors of the mentioned work, since here we are not interested in how realistic is the model or not. The parameter  $\sigma$  characterizes the size of the void. Note that  $\sigma$  has dimensions of length (e.g. Mpc). Such profile is capable of reproducing the  $\Lambda$ CDM distance modulus to high accuracy.

The selection of model 3 of [66] for our analysis does not have a specific motivation. We simply choose the model that the authors find to be the most favored by information criteria (see Table 6 of [66]). This choice always leads to  $\Omega_k > 0$ . As explained in the following section, the selected model does not have relevance in the goal of this work, since we are not interested in putting constraints neither finding the best fits to cosmological models, but to show that certain extra information should be considered when using SNe Ia data that has been analyzed with distinct light-curve fitters.

Since there are still only toy models to describe voids, constructing diagnostics from  $\Lambda$ CDM allow us to visualize what our real constraints on  $\Lambda$ CDM are. Among some quantities that are usually used as non-concordance diagnostics to distinguish between FRW/ $\Lambda$ CDM models and LTB models, we consider the effective deceleration parameter  $q_{\text{eff}}(z)$ , and the effective dark energy equation of state for the void model  $w_{\text{eff}}(z)$ .

These parameters are defined as:

$$q_{\text{eff}}(z) = -1 + \frac{(1+z)}{H_{\parallel}(z)} \frac{d}{dz} H_{\parallel}(z) \quad (16)$$

$$w_{\text{eff}}(z) = \frac{2(1+z)d_c'' + 3d_c'}{3[H_0^2 \Omega_m (1+z)^3 d_c'^2 - 1] d_c'} \quad (17)$$

where in the last equation,  $d_c = (1+z)d_A$  is the comoving angular diameter distance evaluating the void parameters obtained from the best-fitting model to the data, while  $\Omega_m$  and  $H_0$  correspond to the best-fitting to the same data, but in the flat FRW model framework  $\Lambda$ CDM. A prime here means derivative with respect to the redshift  $z$ .

## B. Swiss-cheese model reloaded

Recently, in the work [67], the authors inferred a phenomenological expression for the distance-redshift relation in a Swiss-cheese universe. They found that the

luminosity distance  $d_L = (1+z)^2 d_A^{\text{SC}}$  can be calculated using the heuristic linear combination:

$$d_A^{\text{SC}}(z) = (1-f) d_A^{\text{holes}}(z) + f d_A^{\text{FRW}}(z) \quad (18)$$

where  $d_A^{\text{FRW}}$  is the angular distance for the FRW case,  $d_A^{\text{holes}}$  is given by

$$d_A^{\text{holes}}(z) = \int_0^z \frac{dz'}{(1+z')^2 H(z')} \quad (19)$$

and  $f$  is the *smoothness parameter* defined by

$$f \equiv \lim_{V \rightarrow \infty} \frac{V_{\text{FRW}}}{V} \quad (20)$$

with  $V_{\text{FRW}}$  being the volume occupied by the FRW region within a volume  $V$  of the Swiss-cheese. With this definition,  $f = 1$  corresponds to a model with no hole (i.e. a FRW universe) while  $f = 0$  corresponds to the case where matter is exclusively under the form of clumps. Since here we will consider the flat FRW case with matter ( $\Omega_m$ ) and a cosmological constant ( $\Omega_\Lambda$ ), the Hubble parameter is:  $H(z) = H_0 [\Omega_m(1+z)^3 + \Omega_\Lambda]^{1/2}$ .

In the next section, we will use the LTB model to analyze global effects and degenerations present when SNe Ia observations processed with two different light-curve fitters are used. Then, we will show how the results in the Swiss-cheese model framework are affected.

### III. LIGHT-CURVE FITTERS IN VOID MODELS

In this section, we will use a  $\chi^2$  statistic to analyze the confidence intervals of the free parameters of the two cosmological models introduced before, by employing the same SN Ia data sets, but processed by two different fitters. The three free parameters are, for the LTB model,  $H_0$ ,  $\Omega_{\text{in}}$  and  $\sigma$ ; whilst for the Swiss-cheese model case they are  $\Omega_m$ ,  $H_0$  and  $f$ . Therefore, these models have the same number of free parameters as the curved  $\Lambda$ CDM model cases.

In this work, the analysis was performed in the framework of SALT2 [44] and MLCS [43] fitters and the SN Ia data set used was the SDSSII full data set (Tables 10 and 14 from [5] with the same 'intrinsic' dispersions used there). This data set is, until today, the best one (publicly available) treated and analyzed with both fitters.

As already mentioned, here we are not interested in putting constraints neither in finding the best cosmological model, but to show certain extra information that should be considered when using SNe Ia data processed with different fitters.

We will start considering the LTB model. In Table I, the best-fitting void model parameters derived from SN Ia data are shown. We can observe that while SALT2 has a tendency to give lower values of  $\Omega_{\text{in}}$  and bigger voids, MLCS favors lower values for  $H_0$ . In Fig. 1, we show the confidence intervals at 68.3%, 95.4% and 99.7% in the

$H_0 - \Omega_{\text{in}}$  plane for the SDSSII (MLCS and SALT2) SN Ia data set. There we can see that a tension between the light-curve fitters is present with more than 99.7% confidence level. This was one of the reasons that motivated us to extend our study on inhomogeneous models to the one presented by [42] as we will see further on.

In [66], the authors found that when combining  $H(z)$  data with SN Ia ones for their analysis, the best fit for the size of the void of the model considered here, corresponded to a void 380 Mpc bigger than the one obtained with only SNe Ia data. This behavior was expected, since the fit to  $H(z)$  by itself favors enormous voids. What is interesting is that we found here a variation of around 350 Mpc by just changing the way of processing the same SNe Ia data set. Hence, it seems that an additional uncertainty in  $\sigma$  of about 11% could be associated with the selection of the fitter used. Therefore, when one seeks to constraint the typical size of a void, there seems to exist an extra degeneration between the inclusion of  $H(z)$  data and the fitter employed in the SNe Ia light-curves processing.

TABLE I: Best fits obtained for  $H_0$  (km/s/Mpc),  $\Omega_{\text{in}}$ , and the size of the void  $\sigma$  (Mpc) associated with the LTB model, for the SDSSII (MLCS and SALT2) SNe Ia.

Fitter	$H_0$	$\Omega_{\text{in}}$	$\sigma$
MLCS	63.2	0.24	3050
SALT2	69.2	0.10	3400

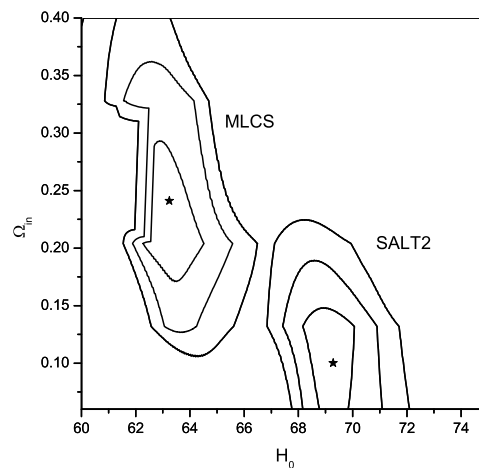


FIG. 1: Confidence intervals at 68.3%, 95.4% and 99.7% in the  $H_0 - \Omega_{\text{in}}$  plane for the SDSSII (MLCS and SALT2) SN Ia data set in the LTB model framework. The best fits are indicated with a star. There can be seen a tension between both processing methods with a confidence level greater than 99.7%. Values of  $H_0$  are expressed in km/s/Mpc.

In [66], the degenerations known between the parameters of these models are discussed. It is mentioned that

to achieve a similar  $\chi^2$ , if one wishes to obtain a bigger void (larger  $\sigma$ ) a lower  $\Omega_{\text{in}}$  is needed; while emptier voids (lower  $\Omega_{\text{in}}$ ) will require a larger  $H_0$ . We will see that the fitters used for the processing of the data lead to similar degenerations.

A work that considered the dependence of the results on the fitter employed, in a inhomogeneous model framework, and with the same SNe Ia set that in the present work, was from the authors of [45]. In Fig. 5 of that work, there can be seen that SALT2 favors values of  $\Omega_{\text{in}}$  lower than those associated with MLCS. Therefore, according to what was mentioned earlier, one would expect that SALT2 would prefer larger voids. And certainly, this is what we found. But we remark that here this is not a consequence of the way these void models are built, but it is a matter of data processing.

We will now analyze the tension between the two light-curve fitters from another perspective. The mentioned degeneration between the parameters  $\Omega_{\text{in}}$  and the size of the void  $\sigma$  can be seen, slightly, in Fig. 2 both for SALT2 and for MLCS.

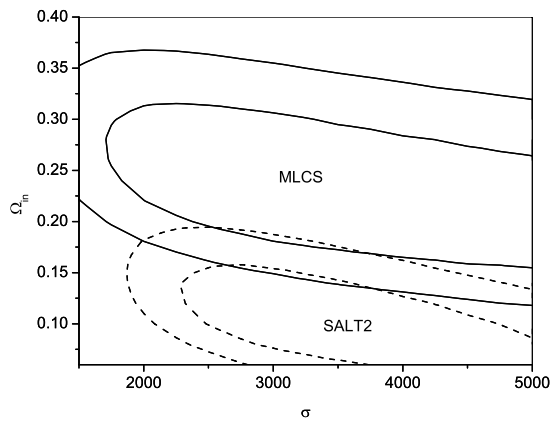


FIG. 2: Confidence intervals at 68.3% and 95.4% in the  $\sigma$ – $\Omega_{\text{in}}$  plane for the SDSSII (SALT2) SNe Ia (dashed lines), and for the SDSSII (MLCS) SNe Ia (solid lines). The  $\sigma$  values are expressed in Mpc.

Let us suppose now that, in the search to find a void for which  $H_0$  is in agreement with the Hubble parameter value found by the *Planck* Collaboration [12] or by the nine years of WMAP [11], we decided to fix the value of  $H_0$  and allow the variation of the two other free parameters. The reader should always have in mind that here we are not interested in the best fits themselves, neither in if the models will be competitive or not. Also, mind that the data is always the same, and the only thing that changes and by which the results become altered, is the way they have been processed. What we would like to address in the following is, how in the very same situation (fixing  $H_0$ ), the *same* data behave in a very different way.

In Table II, we show the best fits to the LTB model having fixed the value of  $H_0$  for the *Planck* and for the WMAP9 cases. The results are surprisingly different. We know that there is a degeneration between  $H_0$  and the void size  $\sigma$ . However, let us note how different it is exhibited when the same data are changed only by the way of processing.

TABLE II: Best fit values having fixed  $H_0$  according to the *Planck* case [12] (67.3 km/s/Mpc) or WMAP9 [11] (70.0 km/s/Mpc). The values of  $\sigma$  are expressed in Mpc.

$H_0$	MLCS		SALT2	
	$\Omega_{\text{in}}$	$\sigma$	$\Omega_{\text{in}}$	$\sigma$
67.3	0.18	1250	0.12	5250
70.0	0.16	750	0.10	2750

In Fig. 4 of [66], the authors show the effect on the distance modulus  $\mu$  for different values of  $H_0$ . They mention that the void parameters they obtained are partially dependent on the value of  $H_0$ . Here, we obtained that the value of  $H_0$  has higher or lower impact depending on the fitter used. For instance, for  $H_0 = 67.3$  km/s/Mpc the best fit for  $\sigma$  between one fitter or the other differs by about 420% and around 370% for the value of WMAP9 (see Table II).

In Fig. 3, we can observe the effect of having fixed  $H_0$ . Both for SALT2 and for MLCS, the degeneration between  $\Omega_{\text{in}}$  and  $\sigma$  appears clearer than in Fig. 2. When  $H_0$  is not fixed, the ellipses of the confidence regions are very large. In particular, for the MLCS case, they are bigger. When fixing the value of  $H_0$ , as it is expected, the confidence regions are reduced giving more restricted values for  $\sigma$ . However, see how in Fig. 3 the ellipse corresponding to the MLCS case is the one which reduces the most, the one which gets the highest impact and in a different way than SALT2. MLCS seems to constraint the values of allowed  $\sigma$  in a more notorious way than SALT2. It can also be appreciated how the confidence intervals for the two fitters in the  $\sigma$  –  $\Omega_{\text{in}}$  plane differ considerably, indicating the tension between both ways of processing the light curves of the SNe.

When we fix the value of  $H_0$  at 70.0 km/s/Mpc [11], the size of the void for the MLCS case is reduced to only 750 Mpc. What we found here is that MLCS would allow the voids not to be giant as it is generally suggested in the literature (even though some authors have shown that giant voids are not mandatory to explain the observations with a LTB model [68]). This is not a conclusive assertion, but something we find interesting to mention as a possible tendency of the data when being processed with MLCS.

Regarding the value of  $H_0$  in the LTB models framework, we would like to leave a concern raised. In the works [69], the author using a local redshift expansion for the luminosity distance and a constraint on the age of the universe, showed that the parameters defining a general LTB model give them enough freedom to enable

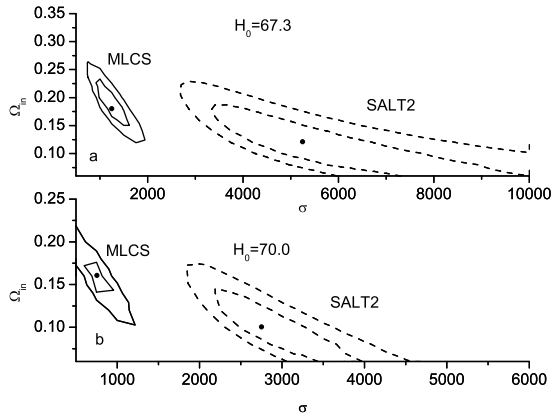


FIG. 3: (a) Confidence intervals at 68.3% and 95.4% in the  $\sigma - \Omega_m$  plane for the SDSSII (SALT2) SNe Ia (dashed lines) and for the SDSSII (MLCS) SNe Ia (solid lines). This case with  $H_0 = 67.3$  km/s/Mpc. (b) Confidence intervals at 68.3% and 95.4% in the  $\sigma - \Omega_m$  plane for the SDSSII (SALT2) SNe Ia (dashed lines) and for the SDSSII (MLCS) SNe Ia (solid lines). This case with  $H_0 = 70.0$  km/s/Mpc. Values of  $\sigma$  are expressed in Mpc, and the best fits are indicated with a dot.

them to agree with any value of  $H_0$ . But if we manage to suit the value of  $H_0$ , we wonder: which SNe light curve processing method should we use to put constraints on the rest of the free parameters of the model? The fitters might give very different values to, for example,  $\Omega_m$  and  $\sigma$ .

We now analyze some quantities that are usually used as non-concordance diagnostics to distinguish between FRW/ $\Lambda$ CDM models and LTB models.

We did not find significant differences between the  $w_{\text{eff}}$  vs.  $z$  curves obtained with SALT2 and MLCS fitters. Nevertheless, in the case of the effective deceleration parameter  $q_{\text{eff}}(z)$ , we did find differences. In Fig. 4, the  $q_{\text{eff}}$  vs.  $z$  curves for both light-curve fitters are shown.

In the MLCS case, we see a more pronounced tendency to a deceleration today than the one found in [66]. Note that the shape of the curve and the deceleration today found by the mentioned authors are very similar to the ones found here under the framework of SALT2 (since both SNe Ia sets are processed with SALT2). Other authors have already found that when the supernovae are processed with MLCS, and then combined with other observations (BAO+CMB+LT) in dark energy models, a case with deceleration today is favored [49].

As mentioned above, the displayed in Fig. 1 in the framework of the chosen LTB model, motivated us to analyze the recent proposal raised in [42] to relieve the tension between the best fits for  $(\Omega_m, H_0)$  derived from SNe Ia data and the ones corresponding to the results of the *Planck* satellite. These authors analyzed the Swiss-cheese model of [67] with the SNLS 3 data set [7] processed with SiFTO/SALT2, and showed that using such

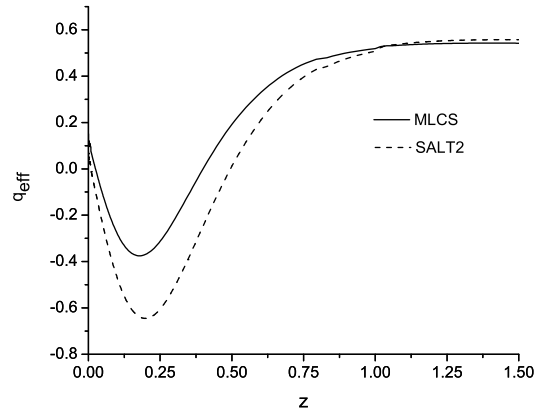


FIG. 4: Curves of the effective deceleration parameter  $q_{\text{eff}}$  vs.  $z$  for the best fit parameters of the LTB model analyzed, to the SNe Ia data processed by SALT2 and MLCS.

inhomogeneous model to interpret the Hubble diagram allows to reconcile it with the *Planck* results. Since SNLS 3 data processed with MLCS are not publicly available, here we will make the study of the same model, but with SDSSII data [5] processed with both SALT2 and MLCS.

Figure 5 shows the confidence intervals at 68.3%, 95.4% and 99.7% in the  $H_0 - \Omega_m$  plane for the SDSSII (MLCS and SALT2) SN Ia data set in the Swiss-cheese model framework of [42, 67].

As we have already mentioned, MLCS favors lower values for  $H_0$  (and larger values for  $\Omega_m$ ) therefore the confidence intervals have been displaced to the left (and up) with respect to the ones for SALT2. Again, with more than 99% confidence level, both light-curve fitters present tension between the obtained results; and our findings suggest that such fitters might play an important role in the results or in the conclusions of proposals such as the ones in [42].

The SNe Ia data of the SDSSII in the framework of a FRW model (case with  $f = 1$  in Fig. 5) do not present tension with the results of *Planck*, and from this point of view, there does not seem to be a need for appealing to an inhomogeneous model to relieve a tension. However, we wonder: could SNLS 3 data processed with MLCS displace to the left as the ones of SDSSII did and achieve a better align with *Planck* when taking into account the suggestion of [42] with  $0 < f < 1$ ? Could a better compatibility between SNe Ia and CMB be achieved following as a guide the search of systematics between MLCS and SALT2 and reducing them? Maybe, the solution found by the authors might be even more reinforced if the most recent SNe Ia data were used in the MLCS fitter framework.

Taking into account the results presented in this work, it is worth making some final reflexions. The community at large uses public data to put constraints on different

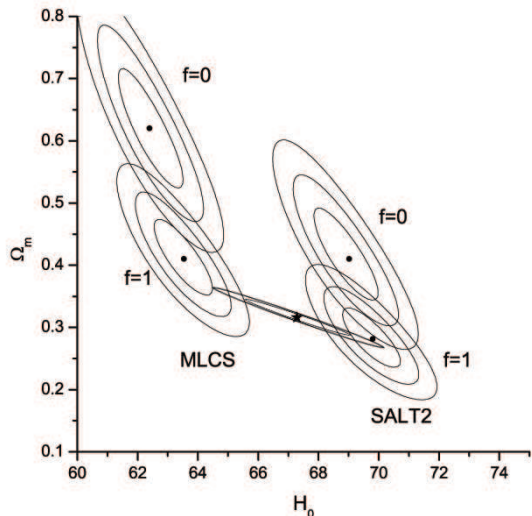


FIG. 5: Confidence intervals at 68.3%, 95.4% and 99.7% in the  $H_0 - \Omega_m$  plane for the SDSSII [5] (MLCS and SALT2) SN Ia data set in the Swiss-cheese model framework. Contour plots with the smoothness parameter  $f = 1$  correspond to the FRW case, whilst the ones with  $f = 0$  correspond to the case where matter is exclusively under the form of clumps. The best fits are indicated with a black dot. Values of  $H_0$  expressed in km/s/Mpc. The best fit of Planck is indicated with a star, and the confidence intervals at 68.3% and 95.4% are also shown. No tension is observed with the data of SDSSII.

proposed models, such as SNLS [7], SDSS [5, 9], Union2 [6], etc., processed with SALT2. It would be useful and interesting to have publicly available the same data, in all cases, also processed with MLCS to be able to use them in carrying out tests to models alternative to  $\Lambda$ CDM. As some authors remarked, the published tables of SNe Ia distance moduli obtained with the SALT/SALT2 fitters retain a degree of model dependence (e.g. flat  $w$ CDM) [48] and should not be applied to constrain other models [51]. In recent years, a great effort has been made to find and study possible sources of systematic errors [10, 52–65], but most of these works are in the framework of SALT2 and we are still not sure if a light-curve fitter is better than the other. In [57], the authors have taken the first steps towards a possible way to detach of the assumed cosmological model dependency in the SALT2 processing; and an interesting study has been made recently with data of the three seasons from the SDSSII and SNLS, comparing results between MLCS and SALT2 [10], but only the distance moduli in SALT2 were published.

#### IV. CONCLUSIONS

In the FRW framework where the universe is isotropic and homogeneous, this is going through an accelerated

stage because of the existence of what we call dark energy. Although the evidence seems to be solid from various observational data sets, the search of other alternatives which also explain these observations have been in development in the last few years. That is the case of the so-called inhomogeneous models. Even though these are toy-models yet and do not accomplish the description of the observations correctly, several authors have remarked the importance of their study, and even in the standard paradigm, some degree of inhomogeneity might have a detectable effect on certain observable quantities.

The luminosity distance measurements of SNe Ia constitute the most used data sets to put observational constraints on cosmological models, since they have been and still are the most solid evidence of the acceleration of the universe detected in the framework of a FRW model. But as it is well known in the standard paradigm, when the same SNe Ia data set is processed with two different light-curve fitters (i.e. SALT2 and MLCS), the values found for cosmological parameters (such as the equation of state  $w$  of dark energy) differ.

In this work, we analyzed the aforementioned difference showing that, similarly to what occurs in the standard model, the light-curve fitters lead to incompatibilities when SNe Ia data are used to put constraints on inhomogeneous models. This can be seen, for instance, in the  $H_0 - \Omega_{in}$  plane in Fig. 1.

We found that when the luminosity fluxes coming from supernovae are processed with the MLCS fitter, the luminosity distances inferred imply sizes of voids 11% smaller than in the SALT2 case. The difference found is of the same order that what other authors obtained [66] when combining SNe Ia data with data of  $H(z)$ . The fitters seem to have a degeneration with these observations. We also showed that SALT2 favors larger voids and lower  $\Omega_{in}$ .

Fig. 1 shows evidence that MLCS favors values of  $H_0$  lower than in the SALT2 case (something that also occurs in the FRW model). This lead us to analyze the proposal of the authors of [42] to relieve the tension in the  $H_0 - \Omega_m$  plane between the values of the *Planck* Collaboration and the one from SNLS 3 SNe Ia data [7]. Although in our work, when using SDSSII data [5], the mentioned tension with *Planck* does not appear, maybe the solution found by those authors might be even more reinforced if the most recent SNe Ia from SNLS data were used in the MLCS fitter framework. We would find interesting the release of more public data sets processed with MLCS to be used in the framework of models alternative to  $\Lambda$ CDM. Note that other authors have warned about the risk of using tables with luminosity distance values in the framework of SALT2 to put constraints on alternative models (e.g. [48, 51]). Given that MLCS constitutes a more model-independent fitter than SALT2, data processed with the former fitter should be preferentially chosen to put constraints to alternative models when using SN Ia data. Alternatively, it would be interesting to have luminosity distances tables in the framework of proposals like the one developed in [57].

We found that MLCS tends to favor an effective deceleration today ( $q_{\text{eff}} > 0$ ) with more emphasis that the SALT2 case. Other authors have already found these trends, but in the framework of dark energy models [49].

When analyzing cases in which the value of  $H_0$  is fixed (for example, to see what would happen if one would want to make the mentioned value compatible with the one obtained from CMB), as it is expected, the allowed ranges for the size of the void are reduced. But, in the same situation (fixing  $H_0$ ), both fitters lead to very different results although the very same data has been used. Also, for MLCS the ranges associated with the size of the void get more restricted than in the case of SALT2. It is interesting to highlight that the size of the void for MLCS, under this situation, might even be smaller than 1 Gpc; indicating that when using MLCS, the size of the voids

might not need to be so giant as it is usually sustained.

### Acknowledgments

G.R.B. and M.E.D.R. are supported by CONICET (Argentina). G.R.B. acknowledge support from the PIP 2009-112-200901-00594 of CONICET (Argentina) and M.E.D.R. acknowledge support from the PIP 2009-112-200901-00305 of CONICET (Argentina) and the PICT Raices 2011-0959 of ANPCyT (Argentina). We would like also to thank Sean February for his helpful clarifications and Diego Travieso for his early collaboration and interesting discussions.

- 
- [1] S. Perlmutter, et al., Bull. Am. Astron. Soc. **29**, (1997) 1351; Astrophys. J. **517**, (1999) 565;
  - [2] A. G. Riess, et al., Astron. J. **116**, (1998) 1009; Astron. J. **607** (2004) 665.
  - [3] G. Miknaitis, et al., Astrophys. J. **666**, (2007) 674.
  - [4] M. Hicken, et al., Astrophys. J. **700**, (2009) 1097.
  - [5] R. Kessler, et al., Astrophys. J. Suppl. Ser. **185**, (2009) 32.
  - [6] R. Amanullah, et al., Astrophys. J. **716**, (2010) 712.
  - [7] A. Conley, et al., Astrophys. J. Suppl. **192**, (2011) 1.
  - [8] N. Suzuki, et al., Astrophys. J. **746**, (2012) 85.
  - [9] M. Sako, et al., arXiv:1401.3317, (2014).
  - [10] M. Betoule, et al., arXiv:1401.4064, (2014).
  - [11] G. Hinshaw, et al., Astrophys. J. Suppl., **208**, (2013) 19.
  - [12] Planck Collaboration, paper XVI, arXiv:1303.5076, (2013).
  - [13] D. Eisenstein, et al., Astrophys. J. **633**, (2005) 560.
  - [14] W. J. Percival, et al., MNRAS **401**, (2010) 2148.
  - [15] D. Huterer and M. S. Turner, Phys. Rev. **D60**, (1999) 081301.
  - [16] V. Sahni and A. A. Starobinsky, Int. J. Mod. Phys. **D9**, (2000) 373.
  - [17] T. Padmanabhan, Phys. Rep. **380**, (2003) 235.
  - [18] J. Frieman, M. S. Turner and D. Huterer, Annu. Rev. Astron. Astrophys. **46**, (2008) 385.
  - [19] D. Huterer, *The Accelerating Universe*, arXiv:1010.1162.
  - [20] M. P. Dabrowski, Astrophys. J. **447**, (1995) 43; M. P. Dabrowski and M. A. Hendry, Astrophys. J. **498**, (1998) 67.
  - [21] J. F. Pascual-Sanchez, Mod. Phys. Lett. **A14**, (1999) 1539.
  - [22] M.-N. Celerier, Astron. and Astrophys. **353**, (2000) 63.
  - [23] K. Tomita, Astrophys. J. **529**, (2000) 382011; MNRAS **326**, (2001) 287.
  - [24] M.-N. Celerier, New Advances in Physics **1**, (2007) 29.
  - [25] K. Enqvist, Gen. Rel. Grav. **40**, (2008) 451.
  - [26] J. Garcia-Bellido and H. Troels, JCAP **0804**, (2008) 003.
  - [27] S. Alexander, et al., JCAP **09**, (2009) 25.
  - [28] T. Biswas, et al., JCAP **11**, (2010) 030.
  - [29] K. Bolejko, et al., Class. Quantum Grav. **28** (2011) 164002.
  - [30] C. Clarkson, Comptes Rendus Physique, Vol. **13**, Issue 6, (2012) 682.
  - [31] M.-N. Celerier, Astron. and Astrophys. **543**, (2012) A71.
  - [32] W. Valkenburg, et al., MNRAS **438**, (2014) L6.
  - [33] J. Garcia-Bellido and T. Haugbølle, JCAP **09**, (2008) 016.
  - [34] A. Moss et al., Phys. Rev. **D83**, (2011) 103515.
  - [35] N. Brouzakis, et al., JCAP **0702**, (2007) 013.
  - [36] K. Kainulainen and V. Marra, Phys. Rev. **D80**, (2009) 127301.
  - [37] K. Bolejko and M.-N. Celerier, Phys. Rev. **D82**, (2010) 103510.
  - [38] R. C. Keenan et al., Astrophys. J. **775**, (2013) 62.
  - [39] K. Bolejko, Astron. and Astrophys. **525**, (2011) A49.
  - [40] W. Valkenburg, et al., Phys. Dark Univ. **2**, (2013) 219.
  - [41] A. E. Romano, et al., European Physical Journal **C72**, (2012) 2242.
  - [42] P. Fleury, et al., Phys. Rev. Lett. **111**, (2013) 091302.
  - [43] M. M. Phillips, et al., Astrophys. J. **413**, (1993) L105; A. G. Riess, et al., Astrophys. J. **438**, (1995) L17; S. Jha, et al., Astrophys. J. **659**, (2007) 122.
  - [44] J. Guy, et al., Astron. and Astrophys. **466**, (2007) 11.
  - [45] J. Sollerman, et al., Astrophys. J. **703**, (2009) 1374.
  - [46] J. C. Bueno Sanchez, et al., JCAP **11**, (2009) 029.
  - [47] C. Pigozzo, et al., JCAP **08**, (2011) 022.
  - [48] P. R. Smale and D. L. Wiltshire, MNRAS **413**, (2011) 367.
  - [49] L. Zhengxiang, et al., JCAP **11**, (2010) 031.
  - [50] G. R. Bengochea, Phys. Lett. **B696**, (2011) 5; G. R. Bengochea, BAAA, Vol. **55**, (2013) 431.
  - [51] J. A. Frieman, AIP Conf. Proc. **1057**, (2008) 87.
  - [52] M. Sullivan, et al., MNRAS **406**, (2010) 782.
  - [53] M. Sullivan et al., Astrophys. J. **737**, (2011) 102.
  - [54] M. C. March, et al., MNRAS **437**, (2014) 3298.
  - [55] H. Lampeitl, et al., Astrophys. J. **722**, (2010) 566.
  - [56] N. Chotard, et al., Astron. and Astrophys. **529**, (2011) L4.
  - [57] J. Marriner, et al., Astrophys. J. **740**, (2011) 72.
  - [58] R. R. Gupta, et al., Astrophys. J. **740**, (2011) 92; Astrophys. J. **741**, (2011) 127.
  - [59] J. Johansson, et al., MNRAS **435**, (2013) 1680.
  - [60] R. Kessler, et al., Astrophys. J. **764**, (2013) 48.
  - [61] X. Wang, et al., Science **340** issue 6129, (2013) 170.



- [62] S. Wang and Y. Wang, Phys. Rev. **D 88**, (2013) 043511.
- [63] M. Rigault, et al., Astron. and Astrophys. **560**, (2013) A66.
- [64] J. Mosher, et al., arXiv:1401.4065, (2014).
- [65] A. Conley et al. Astrophys. J. **681**, (2008) 482.
- [66] S. February, et al., MNRAS **405**, (2010) 2231.
- [67] P. Fleury, et al., Phys. Rev. **D87**, (2013) 123526.
- [68] M.-N. Celerier, et al., Astron. and Astrophys. **518**, (2010) A21.
- [69] A. E. Romano, arXiv:1105.1864, (2011); A. E. Romano, arXiv:1112.1777, (2011).